Zeolites

Crystal Structure Determination of Zeolite Nu-6(2) and Its Layered Precursor Nu-6(1)**

Stefano Zanardi, Alberto Alberti, Giuseppe Cruciani, Avelino Corma, Vicente Fornés, and Michela Brunelli*

It is widely known that the properties of a zeolite in catalytic or ion-exchange applications depend largely on the crystal structure of the zeolite. When a catalytic process takes place in a porous system with dimensions in the range 3–12 Å, the reaction pathway is strongly influenced by framework geometry and the steric constraints are fundamental for driving the reaction towards the desired products.[1,2]

Even though a few extra-large pore zeolites (with channel delimited by more than twelve tetrahedra) have recently been reported, such as CIT-5,[3] UTD-1,[4] or ECR-34[5] (characterized by apertures of 18-membered rings), there are several possible applications that involve molecules larger than the pore dimensions of the available zeolites. To overcome this limitation, mesoporous molecular sieves MCM-41, MCM-48, and MCM-50, with pore dimensions larger (about 30–100 Å) than those of conventional zeolites have been developed.[6] The alluminosilicates that belong to the mesoporous family M41S have a periodic pore structure (i.e., giving rise to coherent X-ray diffraction), whereas the silica walls are disordered and resemble more the structure of a glass. Unlike conventional zeolites, these materials are not strongly acidic,[7] but they do show promise as supports in other types of catalysts, such as olefin polymerization.[8]

Layered zeolitic materials represent another option for treating large molecules. These materials have an advantage in that they combine the good thermal stability of zeolites with active sites of zeolitic nature easily accessible to reactants. In fact, layered zeolitic materials can be pillared or delaminated to produce high-surface-area materials with a majority of their active sites exposed at the crystal surface.[9–11] Nevertheless, so far, only a few structures of synthetic layered silicates have been reported, mainly for two reasons: 1) solution of the crystal structure by powder diffraction is a very challenging task and the small crystal size typically do not allow single-crystal X-ray diffraction experiments, piperazine silicate EU 19 being the only excellent exception;[12] 2) as a consequence of the stacking disorder, which occurs between the layers, the powder-diffraction patterns of a layered material often suffer from severe peak broadening that precludes structure solution.

Notwithstanding the above difficulties, there has recently been an increased activity in the structure elucidation of layered materials.[13–18] Among these materials, those composed by single zeolite sheets like PREFER are particularly interesting,[16] which after calcination leads to the ordered 3D net of the FER-type zeolite. A very similar behavior was reported for the borosilicate named ERB-1,[19] isostructural to MCM-22, the precursor of which is layered in 2D, and the 3D network is formed upon calcination through the condensation of the silanol groups located on the layer surface. Other examples of layered zeolite precursors are EU 19,[12] precursor of the structurally unknown EU 20,[20] its recently reported analogue MCM-69,[17] and the hydrous layer silicate kanemite, a precursor of the industrial ion exchanger SKS-6.[18]

In the early 1980s, Whittam reported the synthesis of new zeolite materials designated Nu-6(1) and Nu-6(2) by using 4,4′-bipyridyne as a structure-directing agent,[21] at the temperatures of 200 °C Nu-6(1) can be converted to Nu-6(2). A wide range of hydrocarbon-conversion catalysts can be prepared from zeolite Nu-6(1) or Nu-6(2) by ion exchange or impregnation with cations.[21] Such catalysts can find application in different process (e.g., catalytic dewaxing, disproportionation, isomerisation of alkanes and alkyl benzenes) in particular Nu-6(2) showed superior activity as catalyst for xylenes isomerization and the like.[21,22] According to Corma et al., a new delaminated stable zeolite, referred to as ITQ-18, can be obtained after expansion and exfoliation of Nu-6(1).[23] ITQ-18 shows a very-large external surface area,

[*] Dr. S. Zanardi, Prof. A. Alberti, Prof. G. Cruciani
Sez. di Mineralogia, Petrologia e Geofisica
Dip. Scienze della Terra
Università degli Studi di Ferrara
44100 Ferrara (Italy)
Fax: (+39) 053-221-0161
E-mail: zrs@unife.it
Prof. A. Corma, Dr. V. Fornés
Instituto de Tecnología Química, UPV-CSIC
Universidad Politécnica de Valencia
Avda. de los Naranjos s/n
46022 Valencia (Spain)
Dr. M. Brunelli
ID31, ESRF, 6 Rue Jules Horowitz
BP 220, 38043 Grenoble Cedex 9 (France)

[**] We thank the European Synchrotron Radiation Facility (ESRF) for providing beamtime. Special thanks to BM1 (the Swiss-Norwegian Beam Lines) staff for the kind assistance during data collections. Dr. A. Chica is acknowledged for performing catalytic tests. Dr. R. Rizzi (CNR-IC, Bari) and Dr. V. Ferretti (University of Ferrara) are gratefully thanked for the helpful discussions.

 DOI: 10.1002/ange.200460085

which is confirmed by its absorption of pyridine. This property of ITQ-18 is in contrast to that of Nu-6(2), which has a negligible amount of OH groups that can interact with the probe molecule. In the case of ITQ-18, all bridging OH groups are accessible to pyridine.[23]

Although the catalytic performance of these materials has been intensively investigated, no crystal structures elucidations were reported so far.

Herein, we describe the crystal structure determination by using X-ray powder diffraction data and synchrotron radiation source of the layered 4,4′-bipyridyl silicate named Nu-6(1) and its calcined form Nu-6(2), which exhibits a new 3D framework topology.

Synchrotron X-ray powder pattern of the Nu-6(1) material was fully indexed by using the program ITO[24] according to a monoclinc symmetry with the following unit cell parameters: $a = 27.741$, $b = 4.973$, $c = 13.936$ Å and $\beta = 103.72°$ (see Table 1). A careful inspection of the systematic absences revealed that the possible space group was $P2_1/a$ (no. 14 International Tables of Crystallography). The integrated intensities of the as-synthesized compound were extracted by using the method of Le Bail et al.[25] with the GSAS[26] Rietveld program and then introduced in the direct methods program SIR97.[27] Although relabeling of some atoms were necessary, a structural model, in which layers were formed by $[SiO_4]$ and $[SiO_3OH]$ tetrahedra, was readily found. Moreover, a careful examination of the interlayer atoms allowed us to localize fragments of the two crystallographically independent 4,4′-bipyridine molecules (44BPY-1 and 44BPY-2 in Figure 1). Analysis of the Fourier maps and extensive model building were necessary to complete the structural model. The Rietveld refinement was successfully completed in the $P2_1$/a space group. Figure 2 shows the good agreement between calculated and observed X-ray diffraction patterns. Details and parameters used during the X-ray powder-diffraction refinement are reported in the experimental section and in Table 1. Crystal structure of Nu-6(1) can be described by layers of $(Si_6O_{13})_n^{2n-}$ parallel to the (100) plane (see Figure 1), held together by hydrogen bonds to the organic molecule. The unit-cell content of the organic molecules from crystal structure refinement (4 per unit cell) is in satisfactory agreement with that inferred from thermogravimetric determination (about 22.8 % wt) and elemental analysis (C 17.84 %, H 1.59 %, N 4.02 %), which accounted for 3.5 organic molecules per unit cell.

Si–O bond lengths lie between 1.557(8) and 1.677(9) Å; O6 and O13 are the terminal oxygen ions, but their bond lengths do not differ significantly from the other Si–O bond lengths. Concerning the interaction between the silicate layer and the organic molecules, the distances calculated for 44BPY-2 (N1b-O13 = 2.56 Å) indicate a strong hydrogen bond, whereas distances refined for 44BPY-1 (N1-O6 = 2.85 Å) suggest a weaker interaction.

The structure of the silicate layer appears to be very similar to those of the layers previously reported for EU 19

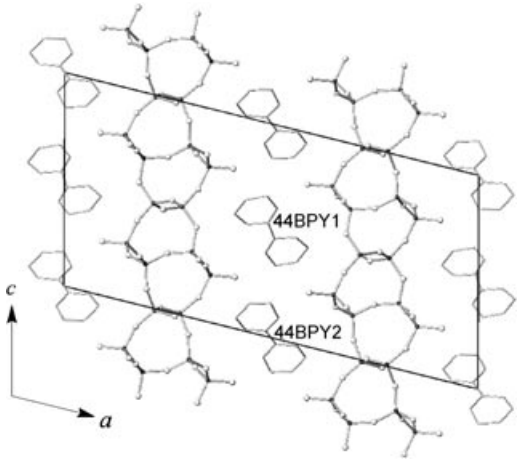

Figure 1. Ball and stick representation of the Nu-6(1) structure along the [010] direction.

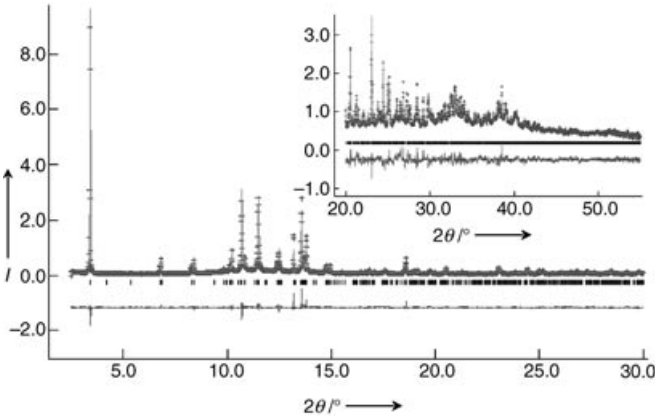

Figure 2. Observed (dotted upper line), calculated (solid upper line), and difference (solid lower line) synchrotron X-ray diffraction patterns of Nu-6(1) in $P2_1/a$.

Table 1: Crystallographic data and experimental conditions for the Rietveld refinement of Nu-6(1) and Nu-6(2).

Sample	Nu-6(1)	Nu-6(2)
chemical formula/unit cell	C40 N8 Si24 O52	Si24 O48
crystal system	monoclinic	
space group	$P2_1/a$	$P2_1/a$
a [Å]	27.7287(6)	17.257(2)
b [Å]	4.9731(1)	4.9881(4)
c [Å]	13.9350(2)	13.848(1)
β [°]	103.73(1)	106.09(1)
V [Å^3]	1866.6(1)	1145.3(2)
X-ray source	synchrotron—BM1B/ESRF	
λ [Å]	0.79982	
refined pattern 2θ range [°]	2.5–55	3.5–40
step size (°2θ)	0.005	
no. of data points	10522	7361
no. of reflections	3714	1375
no. of parameters	137	62
R_F^2 [%]	11.9	7.1
R_p [%]	6.4	4.9
R_{wp} [%]	8.5	6.4
reduced χ^2	9.4	9.7
residual electron density (min/max e Å^{-3})	−0.682/0.915	−0.401/0.438
Durbin–Watson statistics	2.2	2.5

and MCM-69.[12,17] Two out of three cell parameters for Nu-6(1), EU 19, and MCM-69 have the same values (i.e., those of the base dimensions of the sheet); the larger size of the molecules with respect to those hosted in EU 19 and MCM-69 leads to a different stacking parameter, which explains the greater value of a found in Nu-6(1). Moreover the different shape of 4,4′bipyridine is likely to induce a relative shift between the layers, which involves a different symmetry in Nu-6(1) with respect to EU 19 and MCM-69 ($P2_1/a$ instead of $C2/c$).

In the case of Nu-6(2), the quality of the XRD pattern is lower compared with that of the as-synthesized sample because of the concurrent presence of sharp and broad reflections, indicative of a partially disordered structure. Moreover, a pronounced background testifies that, to a certain extent, some layers undergo amorphization upon calcination (Figure 3). To obtain a structural model for Nu-6(2), an approach based on extensive model building was adopted: 1) the crystal structure of the as-synthesized form of Nu-6 was first transformed into a more flexible $P1$ structure; 2) the layers were condensed to form a fully connected 3D framework structure with cell parameters $a \sim 17.25$, $b \sim 4.98$, $c \sim 13.84$ Å and $\beta \sim 106°$; 3) the atomic coordinates in $P1$ space group were introduced in the programme PLATON,[28] which recognized a monoclinic symmetry with standard space group $P2_1/a$. The atomic coordinates were then successfully refined by the Rietveld method (see Figure 3).

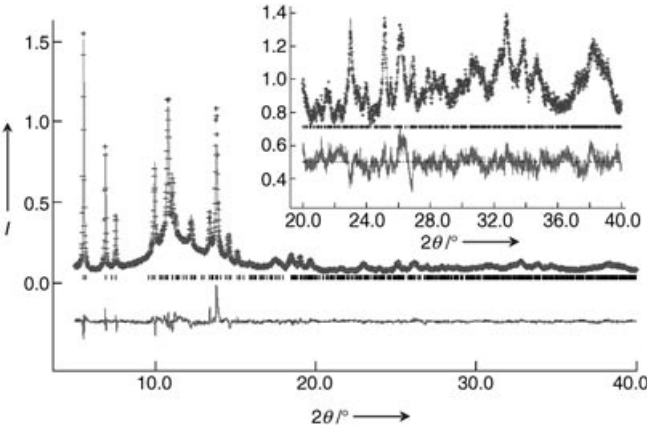

Figure 3. Observed (dotted upper line), calculated (solid upper line), and difference (solid lower line) synchrotron X-ray diffraction patterns of Nu-6(2) in $P2_1/a$.

Figure 4 shows that the framework structure of Nu-6(2) is characterized by the existence of 1D straight eight-membered-ring channels developing along the [010] direction; this feature places Nu-6(2) among the "small pore" zeolites. It must be noted that two non-equivalent sets of eight-ring channels, alternating along the crystallographic c direction, were found in the structure of Nu-6(2); these two sets of channels are referred to as A and B in Table 2, Figure 4 and Figure 5.

It is worth noting the close relationships between the cell parameters refined for Nu-6(2), given in Table 1, and those reported for the orthorhombic cesium aluminosilicate[29] (IZA code CAS) ($a = 13.828(5)$, $b = 16{,}776(5)$ $c = 5.021(1)$ Å). In fact, Nu-6(2) and CAS can be built by applying different symmetry operations to the same pentasil periodic building unit (the layer described above): inversion (i) in the case of Nu-6(2) and reflection (m) in the case of CAS (see Figure 4). However, the different crystal system and the significantly different XRD pattern confirm that the 3D framework topology found in Nu-6(2) has never been reported until now. By considering that the silicate layers

Table 2: Selected distances (Å) across eight-ring channels (see also Figure 5).

	Channel A		
O10–O10	O6–O6	O3–O3	O2–O2
3.6	4.3	4.0	3.2
	Channel B		
O5–O5	O6–O6	O1–O1	O7–O7
2.4	4.8	3.5	3.0

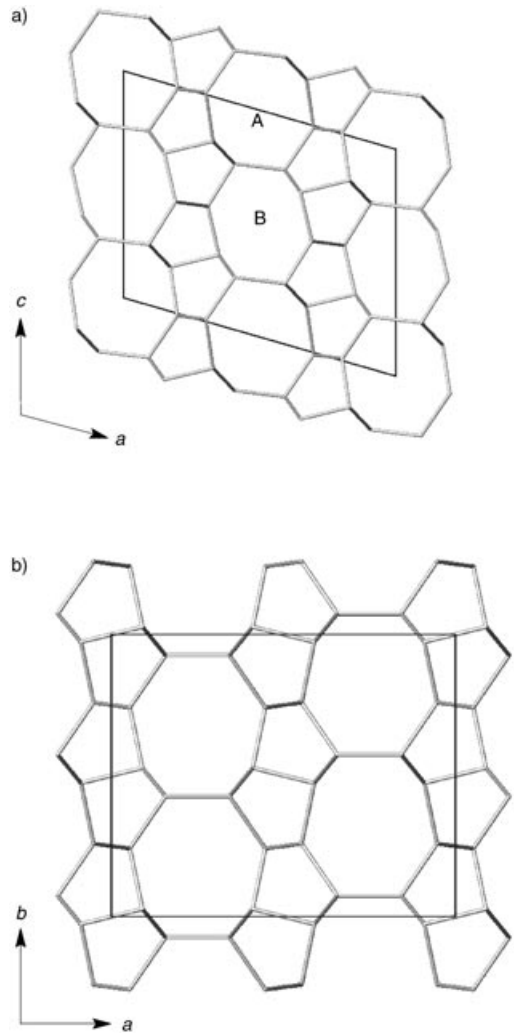

Figure 4. a) Stick representation of the framework structure of Nu-6(2); b) cesium aluminosilicate (IZA code CAS). The two nonequivalent channels, found in Nu-6(2), are labeled A and B.

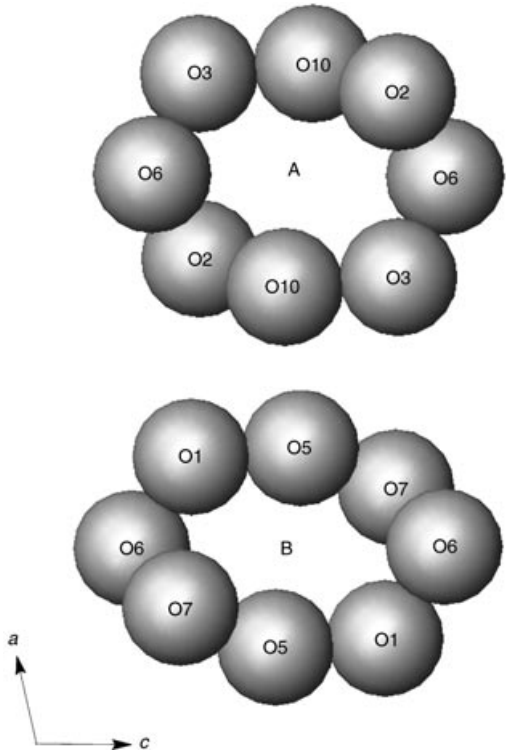

Figure 5. Sphere packing of oxygen atoms defining the A and B eight-ring channels of zeolite Nu-6(2). Please note that channel A and B are alternating along the *c* direction, as evidenced in Figure 4.

comprising EU 19 and Nu-6(1) are isostructural, we can suppose by extension that the structurally unknown EU 20 could have the same topology reported here for the Nu-6(2) structure.

The results of our catalytic tests on hydrocracking of *n*-decane show that Nu-6(2) is an active and selective dewaxing catalyst (see Table 3).

Table 3: Hydrocracking of *n*-decane of a Nu-6(2) zeolite with a Si/Al ratio of 45.

T [°C]	Conv. [%]	Isomerization [%]	Cracking [%]	MB [%][a]	DB [%][a]	NI [%][b]
190	3.8	2.8	1.0	1.6	0.9	0.3
206	10.7	6.2	4.5	3.5	2.3	0.4
221	25.5	9.2	16.3	5.0	3.4	0.8
240	47.8	8.6	39.2	4.5	3.8	0.3
257	70.3	4.8	65.5	2.5	2.2	0.1
270	79.2	3.1	76.1	1.6	1.4	0.1

[a] MB and DB = monobranched and dibranched isomers respectively. [b] NI = non-identified products.

In light of this structural elucidation, we can fully explain the absorption data concerning the pyridine molecule on Nu-6(2);[23] in fact the dimensions of the eight-ring channels are smaller than the pyridine molecule, thus access to the catalytic sites inside the channel is negligible, and the probe molecule can interact only with the bridging OH groups located on the crystal surface.

In conclusion the crystal structure of Nu-6(1) and Nu-6(2) has been determined by using an integrated approach based on experiments and model building. We showed that the structure of precursor 4,4′ bipyridyl silicate is based on a pentasil layer previously recognized in EU 19 and MCM-69; however, the different structure-directing agent used in the synthesis gives rise to a different symmetry and stacking parameter. Moreover, we have demonstrated that upon calcination, silicate layers condense to form a 3D framework structure. The pore topology of this zeolite is unique, with straight eight-membered ring-channel systems along the *b* direction. Finally, *n*-decane hydrocracking catalytic test showed that Nu-6(2) is an active and selective dewaxing catalyst.

Experimental Section

The layered precursor Nu-6(1) was synthesized as follows: 4,4′-bipyridine (1.82 g, 12.3 mmol; Fluka, 98%) were dissolved in ethanol (10.08 g; solution A) while sodium silicate (20.06 g, 0.18 mol; Merck, 24.92% SiO_2) were diluted with water (13.38 g; solution B). Finally, aluminum sulfate (0.62 g, 1.8 mmol; Merck, 51.34%) and of sulfuric acid (1.52 g, 98%) were dissolved in water (22.78 g; solution C) The crystallization was carried out in tumbling teflon-lined autoclaves. After 3 days at 135 °C, the solids were isolated by filtration, washed with distilled water until the pH reached 7, then dried at 60 °C to produce the final Nu-6(1). The 3D Nu-6(2) zeolite was obtained from Nu-6(1) by calcination in air at 550 °C for 6 h.

Catalytic tests on hydrocracking of *n*-decane were performed with Nu-6(2) at atmosphere pressure, contact time of 0.52 h, and molar ration H_2/*n*-decane = 100. Reaction temperature was varied between 190 and 270 °C and the results are given in Table 3.

The high-resolution synchrotron X-ray powder diffraction patterns were collected on the as-synthesized and calcined Nu-6 samples at the beam line BM1B (the Swiss Norwegian Beam Lines), at the synchrotron radiation source ESRF in Grenoble. The beamline provides a robust diffractometer currently equipped with six counting chains, which allows six complete patterns to be collected simultaneously. An Si-111 analyzer crystal is mounted in front of each detector (Na-I scintillation counter). The beam line was set to deliver a wavelength of 0.79982 Å. The samples, placed in a borosilicate capillary 1.0 mm in diameter, were spun during data collection to minimize the preferred orientation. Data were collected, at room temperature, in continuous mode over the range $1 \le 2\theta \le 55°$, with accumulation times increasing with the scattering angle, and rebinned with a step size of 0.005° 2θ.

X-ray powder-diffraction refinement was carried out by using the program GSAS;[25] geometric soft constrain were applied to the Si–O, O–O, C–N and C–C bond length (1.62 ± 0.04, 2.65 ± 0.1, 1.40 ± 0.02, 1.40 ± 0.02 Å, respectively). The weighting factor was gradually reduced as the refinement proceeded and reasonable bond lengths were finally obtained. Atoms of the same element type were constrained to have the same isotropic thermal displacement parameter and refined; only the displacement parameters of the atoms comprising the organic molecules were kept fixed. The occupancies of the organic molecules were refined during the early stage of the refinement; because they did not differ significantly from the unit, they were kept fixed to this value in the final stage of the refinement. Anisotropic broadening phenomena of the reflections were observed in the synchotron X-ray powder diffraction (SXPD) patterns, this phenomenon was accounted

for by including different terms in the pseudo-Voigt peak shape function during the refinements. Further details on the investigation of the crystal structure may be obtained from the Fachinformationszentrum Karlsruhe, 76344 Eggenstein-Leopoldshafen, Germany (fax: (+49) 7247-808-666; e-mail: crysdata@fiz-karlsruhe.de), on quoting the depository numbers CSD-413852 and -413853.

Received: March 22, 2004

Keywords: layered compounds · structure elucidation · X-ray diffraction · zeolites

[1] A. Corma, M. J. Díaz-Cabañas, J. Martínez-Triguero, F. Rey, J. Rius, *Nature* **2002**, *418*, 514.
[2] A. Corma, F. Rey, S. Valencia, J. L. Jorda, J. Rius, *Nat. Mater.* **2003**, *2*, 493.
[3] M. Yoshikawa, P. Wagner, M. Lovallo, K. Tsuji, T. Takewaki, C. Chen, L. W. Beck, C. Jones, M. Tsapatsis, S. I. Zones, M. E. Davis, *J. Phys. Chem. B* **1998**, *102*, 7139.
[4] C. C. Freyhardt, M. Tsapatsis, R. F. Lobo, K. J. Balkus, M. E. Davis, *Nature* **1996**, *381*, 295.
[5] K. G. , Strohmaier, D. E. W. Vaughan, *J. Am. Chem. Soc.* **2003**, *125*, 16035.
[6] J. S. Breck, J. C. Vartuli, W. J. Roth, M. E. Leonowicz, C. T. Kresge, K. D. Schmitt, C. T.-W. Chu, D. H. Olson, E. W. Sheppard, S. B. McCullen, J. B. Higgins, J. L. Schlenker, *J. Am. Chem. Soc.* **1992**, *114*, 10834.
[7] A. Corma, M. S. Grande, V. Gonzalez-Alfaro, A. V. Orchilles, *J. Catal.* **1996**, *159*, 375.
[8] T. Maschmeyer, F. Rey, G. Sankar, J. M. Thomas, *Nature* **1995**, *378*, 159.
[9] A. Corma, V. Fornes, S. B. Pergher, *Nature* **1998**, *396*, 353.
[10] A. Corma, V. Fornes, J. Martinez-Triguero, S. B. Pergher, *J. Catal.* **1999**, *186*, 57.
[11] H. van Olphen, *An Introduction to Clay Colloid Chemistry*, Wiley, New York, **1963**.
[12] S. J. Andrews, M. Z. Papiz, R. McMeeking, A. J. Blake, B. M. Lowe, K. R. Franklin, J. R. Helliwell, M. M. Harding, *Acta Crystallogr. Sect. B* **1988**, *44*, 73.
[13] A. Burton, R. J. Accardi, R. F. Lobo, M. Falcioni, M. W. Deem, *Chem. Mater.* **2000**, *12*, 2936.
[14] U. Oberhagemann, P. Bayat, B. Marler, H. Gies, J. Rius, *Angew. Chem. Int. Ed. Engl.* **1996**, *35*, 2869.
[15] S. , Vortman, J. Rius, S. Siegmann, H. Gies, *J. Phys. Chem. B* **1997**, *101*, 1292.
[16] L. Schreyeck, P. Caullet, J. C. Mougenel, J. L. Guth, B. Marler, *Microporous Mater.* **1996**, *6*, 259.
[17] L. D. Rollmann, J. L. Schlenker, S. L. Lawton, C. L. Cannedy, G. J. Kennedy, *Microporous Mesoporous Mater.* **2002**, *53*, 179.
[18] S. Vortmann, J. Rius, B. Marler, H. Gies, *Eur. J. Mineral.* **1999**, *11*, 125.
[19] R. Millini, G. Perego, W. O. Parker, Jr., G. Bellussi, L. Carluccio, *Microporous Mater.* **1995**, *4*, 221.
[20] A. J. Blake, K. R. Franklin, B. M. Lowe, *J. Chem. Soc. Dalton Trans.* **1988**, 2513.
[21] T. V. Whittam, US Pat. 4 397 825, **1983.**
[22] I. J. S. Lake, T. V. Whittam, US Pat. 4 400 572, **1983.**
[23] A. Corma, V. Fornés, U. Diaz, *Chem. Commun.* **2001**, 2642.
[24] J. W. Visser, *J. Appl. Crystallogr.* **1969**, *2*, 89.
[25] A. , LeBail, H. Duroy, J. L. Fourquet, *Mater. Res. Bull.* **1988**, *23*, 447–452.
[26] A. C. Larson, R. B. Von Dreele, GSAS Manual, Los Alamos Report No. LAUR-86–748, Los Alamos National Laboratory, USA, **1986**.
[27] A. Altomare, M. C. Burla, M. Camalli, G. L. Cascarano, C. Giacovazzo, A. Guagliardi, A. G. G. Moliterni, G. Polidori, R. Spagna, *J. Appl. Crystallogr.* **1999**, *32*, 115.
[28] A. L. Spek, *Acta Crystallogr. Sect. A* **1990**, *46*, C34.
[29] T. Araki, *Z. Kristallogr.* **1980**, *152*, 207.

